

## A Protein Biosensor That Relies on Bending of Single DNA Molecules

Robert Crawford,<sup>[a]</sup> Douglas J. Kelly,<sup>[b]</sup> and Achillefs N. Kapanidis<sup>\*,[a]</sup>

Transcription factors (TFs) form an important class of DNA-binding proteins that control gene expression. Sequence-specific TF binding to DNA in response to environmental stimuli modulates promoter binding by RNA polymerase (RNAP) and transcription of specific genes.<sup>[1]</sup> As a result, the ability to rapidly detect and quantify the concentration of TFs and their response to stimuli will help understand regulatory mechanisms and provide important tools for diagnostics and drug discovery. Detection of TFs is often achieved through western blots or ELISAs, whereas their binding sites can be identified using chromatin precipitation methods such as ChIPseq.<sup>[2]</sup> These methods provide a good overview of ensemble TF levels in a cell population but they are laborious, time-consuming, require large amounts of sample and miss variations at the single-cell level. More recently, GFP-tagging has been employed to quantify distributions of total concentrations of a wide variety of proteins, including many TFs, at the single-cell level but unfortunately cannot distinguish between active and inactive TFs.<sup>[3]</sup>

An important mechanism by which many prokaryotic and eukaryotic TFs modulate transcription is by DNA bending. DNA bending can act to bring distal DNA elements into close proximity to promote interactions between other TFs or with the transcription machinery itself.<sup>[4]</sup> TF-induced bending can also help RNAP discriminate between promoter and non-promoter sequences by enabling an induced-fit mechanism.<sup>[5]</sup> Therefore, methods that detect protein-mediated DNA bending can serve as an avenue for TF detection; however, such methods are underdeveloped. Electrophoretic mobility shift assays such as circular permutation or cyclization analysis are used to infer bend angles from shifts caused by protein binding site variations, but have low sensitivity.<sup>[6]</sup> Bending is identified using the combined effect of TF binding to multiple sites along a long DNA segment. Force-based single-molecule approaches such as tethered particle motion, atomic force microscopy and magnetic tweezers have been used to study the formation of DNA looping caused by individual repressor proteins binding (and bending) two or more operator sites.<sup>[7]</sup> Thermodynamics of loop formation under different conditions including additional DNA-bending cofactors have been explored, however the

method has not been used to detect protein-induced bends at individual binding sites.

The ability to distinguish individual protein-DNA bending events is suited to single-molecule approaches that report on local, nanometer-scale changes. Recently, we demonstrated single-molecule TF detection using TF-mediated molecular 'coincidence' of two DNA half-sites,<sup>[8]</sup> an observable made possible using alternating laser excitation (ALEX).<sup>[9]</sup> While this system allowed accurate TF quantification, no information on the TF-induced DNA bend was available. However, the second ALEX observable, Förster resonance energy transfer (FRET) efficiency, can report on distance changes due to DNA bending. FRET, a 'spectroscopic ruler', is a photophysical interaction reporting on the distance between a 'donor' and 'acceptor' dye, as long as it is within the 1–10 nm range.<sup>[10]</sup> This range limits the use of linear DNA segments to sense TF-mediated DNA bending using FRET, since such sensing would either require TF targets exhibiting extremely large bend angles ( $> 110^\circ$  for a 40-mer with a 10 bp binding site),<sup>[11]</sup> or fluorophores placed close to the protein binding site or on the protein itself.<sup>[12]</sup> Here we describe a FRET-based sensor that detects the presence of an active, unmodified TF via amplification of DNA bending. The assay can be used for ensemble and single-molecule *in vitro* measurements on surfaces and in solution. Such a construct could also be used *in vivo*, considering that FRET has been used for sensing small molecules and pH changes in cells.<sup>[13]</sup>

To build a FRET-based bending sensor made of DNA, we extended a strategy that uses sequence-directed DNA kinks to bring the ends of a long DNA within the dynamic range for FRET.<sup>[14]</sup> We characterize the sensor sensitivity, selectivity, and versatility at the single-molecule level, allowing direct observation of any heterogeneity.

The DNA sensor is a double-stranded DNA fragment consisting of one 72-mer and one 68-mer that, when annealed, forms three five-adenine ( $A_5$ ) 'kinks' and a binding site for the TF target. The target used was catabolite activator protein (CAP), a global regulator that causes a DNA bend angle of  $\sim 80\text{--}90^\circ$  (Figure 1a).<sup>[12b,15]</sup> The  $A_5$  kinks, containing 5 unpaired adenine bases, introduce specific bends within a DNA structure through sequence-directed curvature alone; the solution structure of an  $A_5$  kink indicates a DNA bend angle of  $73^\circ (+/-11^\circ)$ .<sup>[16]</sup> Three  $A_5$  kinks placed at specific points along the DNA sensor allow the two ends of the DNA to be brought within the range of FRET that would otherwise be spaced  $> 20$  nm apart. Edge lengths were designed such that the DNA sensor molecule is folded on the same plane.<sup>[14]</sup> The 5' end of the 'top' strand of the sensor was labelled with a FRET donor (Cy3B) and the 3' end with a biotin tag for surface attachment; the 5' end of the

[a] Dr. R. Crawford, Dr. A. N. Kapanidis  
Biological Physics Research Group  
Clarendon Laboratory, Department of Physics  
University of Oxford, Parks Road, Oxford (UK)  
E-mail: a.kapanidis1@physics.ox.ac.uk

[b] D. J. Kelly  
Institute of Chemical Biology (ICB)  
Imperial College London  
South Kensington Campus, London (UK)

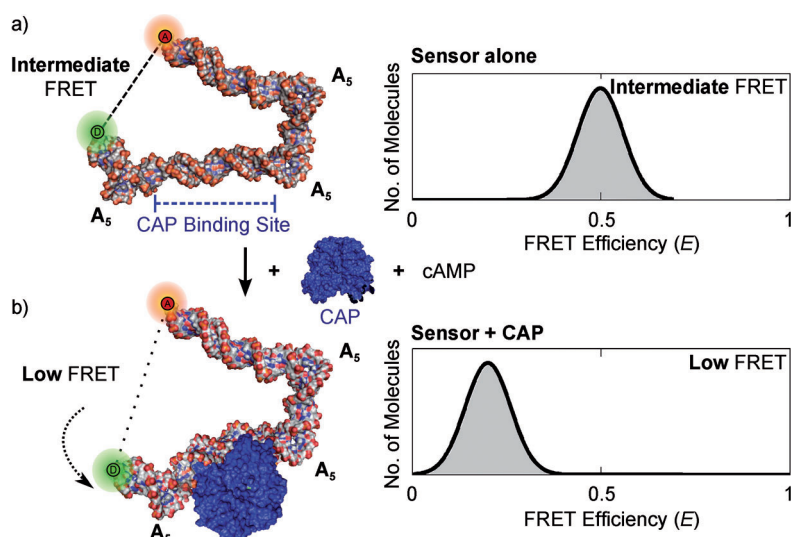


**Figure 1.** A FRET-based TF sensor based on DNA bending. a) Left: the sensor consists of a single dsDNA containing three  $A_5$  kinks and a TF binding site (here, the TF is CAP) placed along one edge. A donor (green) is placed at one end of the sensor and an acceptor (red) at the other. Right: the proximity of the fluorophores in the unbound state close to the Förster distance ( $R_0$ ) yields an intermediate FRET population. b) Left: in the presence of CAP (and the co-factor cAMP), the protein binds to and bends the sensor, pulling the ends of the sensor apart. Right: the increased donor–acceptor distance results in lower FRET population. Schematics use PDB structures 1CGP (CAP–DNA complex) and 1QSK ( $A_5$  kink).<sup>[15–16]</sup>

‘bottom’ strand of the sensor was labelled with a FRET acceptor (ATTO647N).

The sensing strategy depends on changes in FRET efficiency within the DNA sensor as a result of the presence of the target protein, CAP. In the absence of CAP, the ends of the sensor are spaced close to the characteristic Förster distance ( $R_0$ ) for the donor–acceptor pair resulting in an intermediate FRET efficiency and high sensitivity to distance changes (Figure 1a). In the presence of CAP, the protein binds to the sensor along one edge, inducing DNA bending, and causing the ends of the sensor to move further apart, decreasing the FRET efficiency (Figure 1b).

To probe the response of the sensor to CAP, we used solution-based single-molecule FRET confocal measurements combined with ALEX,<sup>[17]</sup> we incubated 50 pM sensor DNA with 0–600 nM active CAP dimer and 0.2 mM cofactor cyclic AMP (see Experimental Section). Molecules were excited using alternating green light (that primarily excites the donor) and red light (that excites the acceptor), allowing molecular sorting on the basis of apparent FRET efficiency,  $E^*$ , and relative probe

the binding site, as well as the binding buffer conditions.

Surface-based approaches for TF detection allow rapid parallel detection of many molecules at once, thus enabling multiplexing. To test sensor compatibility with solid supports, we immobilized it on a glass surface via a biotin/neutravidin linkage and probed the FRET response using total internal reflection fluorescence microscopy (TIRF) combined with ALEX. We

stoichiometry,  $S$ .<sup>[18]</sup> The FRET distribution for the sensor alone revealed the presence of two FRET peaks: a major FRET peak at  $E^* \sim 0.40$  and a low-FRET peak at  $E^* \sim 0.25$  (Figure 2a); upon increasing CAP concentration, most of the 0.4  $E^*$  species is converted to the low-FRET state, reflecting the fact that the sensors are bound by CAP and bent. Fitting the distribution to a double Gaussian and plotting the relative area under the first peak leads to the determination of the dissociation constant,  $K_D$ , of  $\sim 58$  nM (Figure 2b), a value in good agreement with ensemble-FRET results ( $\sim 30$  nM; not shown). The affinity of the target protein for the sensor will determine the sensitivity and detection limit of the assay; the latter can be tuned by modifying the sequence or length of

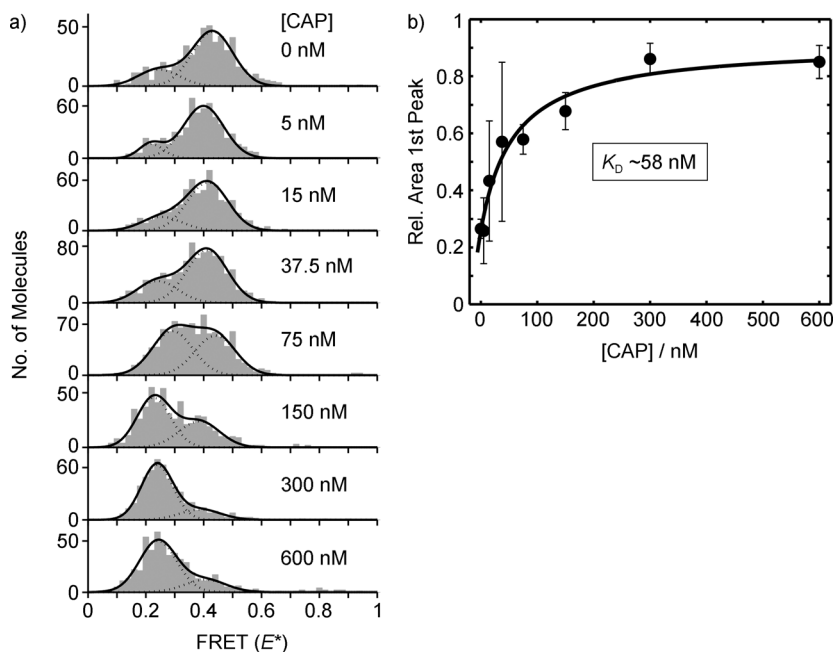


**Figure 2.** Sensing CAP at the single-molecule level through DNA bending: a) FRET distributions for doubly labelled molecules as a function of CAP concentration. Each distribution is fitted to a double Gaussian. b) Fitting the increase in the occupancy of the low-FRET peak to the Hill equation yields a  $K_D$  of  $\sim 58$  nM (error bars:  $\pm$  SEM).

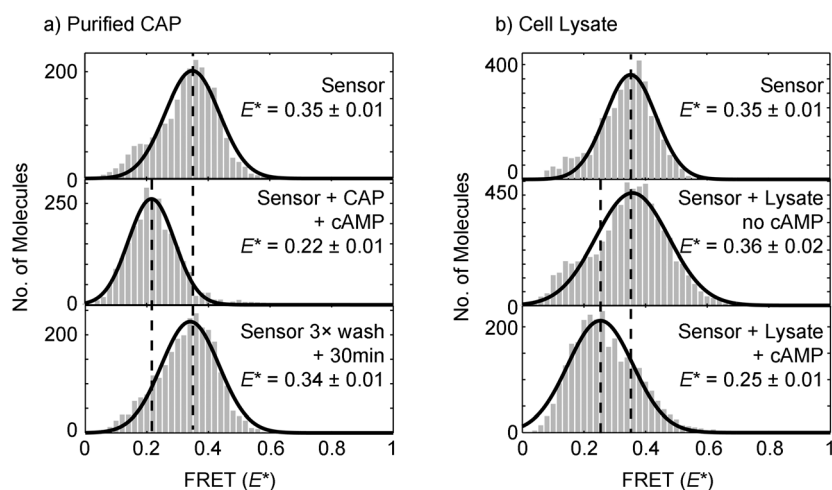


**Figure 3.** Single-molecule surface-based detection of CAP in purified form or expressed in a cell lysate. Shown are the uncorrected FRET distributions ( $E^*$ ) for double-labeled molecules. a) Testing the sensor with purified CAP. Top: the sensor itself in binding buffer exhibits an  $E^*$  value of  $0.35 \pm 0.01$ . Middle: addition of  $1.2 \mu\text{M}$  active CAP dimer and  $0.2 \text{ mM}$  cAMP results in a drop in  $E^*$  to  $0.22 \pm 0.01$  corresponding to binding and bending by CAP. Bottom: washing the sensor three times in binding buffer and incubation for 30 min results in  $E^*$  returning to  $0.34 \pm 0.01$ , enabling sensor re-use. b) Testing the sensor in a cell lysate. Top: the sensor itself measured again in binding buffer exhibits an  $E^*$  value of  $0.35 \pm 0.01$ . Middle: addition of  $10 \text{ mg mL}^{-1}$  *E. coli* lysate containing expressed CAP but without additional cyclic AMP (cAMP) results in no major change in  $E^*$  ( $0.36 \pm 0.02$ ), as expected. Bottom: further addition of  $0.2 \text{ mM}$  cAMP results in a drop in  $E^*$  to  $0.25 \pm 0.01$ , demonstrating the sensor's specific response to CAP.

first probed the response of the immobilized sensor to purified CAP. Without CAP, the sensor yields an uncorrected FRET efficiency ( $E^*$ ) of  $0.35 \pm 0.01$  (Figure 3a, top); the absence of a significant low-FRET subpopulation indicates that the two populations seen in confocal measurements ( $\sim 1$  ms time resolution) may be dynamically interconverting during the 50 ms exposure time of TIRF measurements.

Addition of  $1.2 \mu\text{M}$  active CAP dimer and  $0.2 \text{ mM}$  cyclic AMP to the immobilized sensors bends the DNA and decreases the mean  $E^*$  to  $0.22 \pm 0.01$  (Figure 3a, middle; see also Experimental section). At this concentration, the sensors should be  $>99\%$  bound (considering the  $K_D$  of  $\sim 58 \text{ nM}$ ). We also showed that the sensor was reusable: washing the sensor three times with binding buffer and incubating for 30 min allowed dissociation of CAP and a return to the  $E^*$  of free DNA ( $0.34 \pm 0.01$ ; Figure 3a, bottom).

Whilst changes in  $E^*$  report reliably on relative FRET changes and are sufficient for biosensing purposes, the exact  $E^*$  values depend on factors such as crosstalk contributions (donor leakage, acceptor direct excitation) and differences in detection efficiency and quantum yield of the fluorophores.<sup>[19]</sup> However, if we correct for these factors (see Experimental Section), we recover a donor-acceptor distance of  $\sim 72 \text{ \AA}$  ( $E \sim 0.29$ ) in the unbound state of the sensor. Using a simple structural model that assumes a B-DNA geometry for the four helical segments and in-plane bending, the measured distance corresponds to an angle of  $\sim 69^\circ$  per  $A_5$  kink, in good agreement with reported values of  $\sim 73^\circ$ .<sup>[16,20]</sup> Upon CAP binding, this distance increases to  $\sim 88 \text{ \AA}$  ( $E \sim 0.11$ ), consistent with bending of the donor-proximal helical segment away from the acceptor. Although it is not possible to estimate reliably the degree of CAP-induced bend-

ing (especially considering the presence of FRET heterogeneity seen in our confocal data), methods to characterize DNA deformation using single-molecule FRET methods are available.<sup>[20]</sup>

We then tested the robustness of the sensor response in a complex biological sample. For this experiment, an *E. coli* cell lysate containing highly expressed CAP (where it constitutes  $\sim 20\text{--}30\%$  of total cell protein, that is,  $\sim 300 \mu\text{M}$  CAP dimer)<sup>[8]</sup> was prepared. Consistent with the previous experiment, the free sensor yields an  $E^*$  of  $0.35 \pm 0.01$  (Figure 3b, top). The lysate was then added at a concentration of  $10 \text{ mg mL}^{-1}$  but with no additional cyclic AMP (cAMP); since cAMP is required by CAP to bind to its recognition sequence,<sup>[21]</sup> it proved a useful

tool in evaluating the sensor performance in lysates. Endogenous cAMP from the lysate does not affect binding, since intracellular cAMP concentrations are  $\sim 0.5\text{--}10 \mu\text{M}$  ( $\sim 15\text{--}330 \text{ nM}$  after the dilution during lysate preparation),<sup>[21]</sup> far below the optimum for CAP-DNA binding ( $\sim 0.2 \text{ mM}$ ). In the lysate, the sensor appears to be robust since the mean  $E^*$  for the sensor is largely unaffected ( $0.36 \pm 0.02$ ; Figure 3b, middle); the broadening of the distribution may reflect either weak binding activity of CAP at  $\text{cAMP} < 30 \mu\text{M}$  or other non-specific DNA-processing proteins.<sup>[22]</sup> Finally, adding  $0.2 \text{ mM}$  cAMP to the lysate mix decreased  $E^*$  to  $0.25 \pm 0.01$  (a value similar to the one using purified CAP), highlighting the sensor's specific response to CAP (Figure 3b, bottom).

Our proof-of-concept experiments can be extended to other DNA-bending proteins by inserting the specific binding site for the protein of interest. For example, important TFs such as NF- $\kappa$ B (involved in immune response), SRY (sex determination) and Sox2 (cell differentiation) bend DNA by  $75\text{--}110^\circ$ ,  $83^\circ$  and  $80^\circ$  respectively,<sup>[23]</sup> and should be easily detectable using similar DNA sensors. Multiplexed detection of several DNA-bending TFs could be performed using spatial or spectral separation. Spectral separation could be achieved using different FRET (E) or stoichiometry (S) codes for each target, either by fluorophore placement, different inherent bend angle, or use of multiple fluorophores.<sup>[24]</sup> Modifications of binding sequence could be used to detect different concentration ranges of protein. For example, for our CAP assay, we used the wild-type binding sequence which has  $\sim 450$ -fold lower affinity than for the consensus site;<sup>[25]</sup> the latter can be used to detect much lower concentrations. The time-to-result for our proposed assay is  $\sim 15$  min (including sample incubation and data analysis).

While incubation times could be further shortened, the current time-to-result is significantly shorter than alternative methodologies such as ELISAs, chromatin precipitation or PCR-based assays which can take hours to produce a result.<sup>[2,26]</sup>

Finally, a DNA-bending sensor introduced into the bacterial cytoplasm would be able to directly report on active TF concentration changes in vivo; methods to introduce short, fluorescent, degradation-resistant DNAs into bacteria are under development (Crawford et al., in preparation) and should turn this exciting possibility into reality.

## Experimental Section

### Formation of the DNA Sensor

The oligonucleotides used were ordered from Integrated DNA Technologies. Sequences are given 5' → 3'. Top strand: C6Amine CC CAC TGC CGA ATG TGA GTT AGC TCA CTC ACG AAA AAC CAC TGT CGA AAA AGC TCT ACG GGC TCT GGC GTC GG Biotin. Bottom strand: C6Amine CC GAC GCC AGA GCC CGT AGA GCC GAC AGT GGC GTG AGT GAG CTA ACT CAC ATT CGA AAA AGC AGT GGG.

Labeling at the 5'-end of oligonucleotides was performed using the 5'-amino-C6-modifying group with N-hydroxy-succinimidyl esters of Cy3B (GE Healthcare, Uppsala, Sweden) or ATTO647N (ATTO-TEC GmbH, Siegen, Germany) using manufacturer's instructions, and were PAGE-purified. Oligos were annealed together to form the DNA sensor in annealing buffer (20 mM Tris-HCl (pH 8.0), 500 mM NaCl, 1 mM EDTA) by heating to 94 °C and subsequent cooling to 4 °C over 2 h in steps of 1 °C.

### Confocal Experiments

50 pM of DNA sensor were incubated with 0–600 nM active CAP dimer in binding buffer (20 mM HEPES-NaOH (pH 7), 100 mM potassium-L-glutamate, 200 mM NaCl, 1 mM DTT, 100 μg mL<sup>-1</sup> BSA, 1 mM MEA, 5% glycerol) and in the presence of 0.2 mM cAMP for 10 min at room temperature. The incubated mixture was examined and analyzed as in.<sup>[8]</sup> Data fitting for FRET distributions and the  $K_D$  (Hill equation) were performed using MATLAB.

### TIRF Experiments

50 pM of biotinylated DNA sensor was immobilized on a glass coverslip coated with PEG-Biotin and PEG (1.25:100 ratio) after it had been incubated with 0.5 mg mL<sup>-1</sup> neutravidin for ~3 min. The protocols for slide cleaning and immobilization of biotinylated DNA have previously been described.<sup>[17a]</sup> Binding reactions with CAP took place on the coverslip. DNA sensors were incubated with CAP in binding buffer (as above) for 10 min at room temperature. Binding buffer was supplemented with or without 0.2 mM cAMP as described in the main text. TIRF measurement apparatus was the same as previously described.<sup>[8]</sup> Each measurement consisted of 1 s movies with 20 Hz frame rate. For each sample, a total of ~30 movies were collected. FRET values were calculated for individual double-labelled molecules from an average of 2 frames per movie and plotted on an  $E^*$ - $S$  histogram. The data was then collapsed onto one-dimensional  $E^*$  histograms, as shown in Figure 2. Data analysis was performed on home-built software made with MATLAB.

### Purified CAP

CAP was prepared essentially as previously described.<sup>[27]</sup> CAP activity was determined by electrophoretic shift assay (EMSA) to be ~30%.

### Bacterial Lysates Containing Expressed CAP

*Escherichia coli* BL21(DE3) carrying plasmid pAKCRP was grown in 100 mL fresh LB at 37 °C to an OD<sub>600</sub> of ~0.4. The culture was then induced with 1 mM IPTG and grown for a further 3 hrs. Cells were collected by centrifugation, the supernatant discarded and pellet resuspended in KGE buffer (20 mM HEPES-NaOH pH 7.0, 100 mM potassium-L-glutamate, 1 mM DTT, 100 mg mL<sup>-1</sup> BSA, 1 mM MEA, 10 mM EDTA, 5% glycerol and supplemented with Roche Complete Protease Inhibitor). Cells were sonicated six times (30 s on, 30 s ice) and cell debris removed by centrifugation at 30000 g for 20 min. Protein in the supernatant was quantified using 280 nm absorption.

### Accurate FRET Measurements

For donor-only molecules ( $S > 0.9$ ), we calculate a leakage value of  $l = 0.14$  and for acceptor-only molecules ( $S < 0.2$ ), we calculate a direct excitation value of  $d = 0.035$ . Gamma was assumed to be one for this sample. The  $R_0$  value for the Cy3B-Atto647N pair was calculated using the spectra and donor quantum yield for the free dyes, and was found to be ~62 Å. The steady-state anisotropy for the Cy3B and ATTO647N fluorophores attached to the sensor are 0.2 and 0.23, respectively, showing the presence of substantial rotational freedom for the fluorophores and justifying the assumption that the orientation factor  $\kappa^2$  is close to its isotropic averaging value of 2/3.

### Structural Model

We considered four helical segments of length 74.8 Å (22 bp), 30.6 Å (9 bp), 81.6 Å (24 bp), and 27.2 Å (8 bp) for segments named 1–4, respectively.  $A_5$  kinks of unknown bend angle connected segments 1–2, 2–3, and 3–4. The distance between the sensor ends was calculated from accurate FRET measurements to be 72 Å (see main text). Assuming the helical segments lie in the same plane,<sup>[14]</sup> geometric considerations for a two-coordinate system ( $x, y$ ) allowed formation of two equations for the two unknowns: the  $A_5$  kink angle, and the angle between the ends of the sensor. The equations used were [Eqs. (1) and (2)]:

$$74.8 + 30.6 \cos(\pi - x) - 81.6 \cos(3\pi/2 - 2x) - 27.2 \cos(2\pi - 3x) - 72.1 \cos(p) = 0 \quad (1)$$

$$-30.6 \sin(\pi - x) - 81.6 \cos(3\pi/2 - 2x) + 27.2 \sin(2\pi - 3x) + 72.1 \sin(p) = 0 \quad (2)$$

where  $(\pi - x)$  gives the  $A_5$  kink angle, and  $p$  is the angle between the ends of the sensor. Solving Equations (1) and (2) gives:  $x \approx 1.94(111^\circ)$ ,  $p \approx 1.55(89^\circ)$ . The  $A_5$  kink angle was therefore determined to be ~69°.

### Acknowledgements

We thank Kristofer Gryte and Johannes Hohlbein for help with data analysis. R.C. was supported by a PhD Plus scholarship (EPSRC) and St John's College, Oxford University. A.N.K. was sup-



ported by a European Commission Seventh Framework Program grant (FP7/2007–2013 HEALTH-F4–2008–201418) and a UK BBSRC grant (BB/H01795X/1).

**Keywords:** biosensing · detection · DNA bending · single-molecule studies · transcription factor

- [1] C. Branden, J. Tooze, *Introduction to Protein Structure*, Garland Publishing, New York, 1999.
- [2] G. Robertson, M. Hirst, M. Bainbridge, M. Bilenky, Y. Zhao, T. Zeng, G. Euskirchen, B. Bernier, R. Varhol, A. Delaney, N. Thiessen, O. L. Griffith, A. He, M. Marra, M. Snyder, S. Jones, *Nat. Methods* **2007**, *4*, 651–657.
- [3] Y. Taniguchi, P. J. Choi, G.-W. Li, H. Chen, M. Babu, J. Hearn, A. Emili, X. S. Xie, *Science* **2010**, *329*, 533–538.
- [4] P. C. van der Vliet, C. P. Verrijzer, *BioEssays* **1993**, *15*, 25–32.
- [5] G. Tang, A. P. Deshpande, S. S. Patel, *J. Biol. Chem.* **2011**, *286*, 38805–38813.
- [6] a) H.-M. Wu, D. M. Crothers, *Nature* **1984**, *308*, 509–513; b) D. Kotlarz, A. Fritsch, H. Buc, *The EMBO Journal* **1986**, *5*, 799–803.
- [7] L. Finzi, D. D. Dunlap, *J. Biol. Chem.* **2010**, *285*, 18973–18978.
- [8] K. Lympopoulos, R. Crawford, J. Torella, M. Heilemann, L. C. Hwang, S. J. Holden, A. N. Kapanidis, *Angew. Chem.* **2010**, *122*, 1338–1342; *Angew. Chem. Int. Ed.* **2010**, *49*, 1316–1320.
- [9] A. Kapanidis, T. Laurence, N. K. Lee, E. Margeat, X. Kong, S. Weiss, *Acc. Chem. Res.* **2005**, *38*, 523–533.
- [10] L. Stryer, R. P. Haugland, *Proc. Natl. Acad. Sci. USA* **1967**, *58*, 719–726.
- [11] S. V. Kuznetsov, S. Sugimura, P. Vivas, D. M. Crothers, A. Ansari, *Proc. Natl. Acad. Sci. USA* **2006**, *103*, 18515–18520.
- [12] a) T. Heyduk, E. Heyduk, *Nat. Biotechnol.* **2002**, *20*, 171–176; b) A. N. Kapanidis, Y. W. Ebricht, R. D. Ludescher, S. Chan, R. H. Ebricht, *J. Mol. Biol.* **2001**, *312*, 453–468.
- [13] a) B. Ponsioen, J. Zhao, J. Riedl, F. Zwartkruis, G. v. d. Krogt, M. Zaccolo, W. H. Moolenaar, J. L. B. K. Jalink, *EMBO Rep.* **2004**, *5*, 1176–1180; b) S. Modi, M. Swetha, D. Goswami, G. D. Gupta, S. Mayor, Y. Krishnan, *Nat. Nanotechnol.* **2009**, *4*, 325–330.
- [14] F. Stühmeier, A. Hillisch, R. M. Clegg, S. Diekmann, *J. Mol. Biol.* **2000**, *302*, 1081–1100.
- [15] S. C. Schultz, G. C. Shields, T. A. Steitz, *Science* **1991**, *253*, 1001–1007.
- [16] U. Dornberger, A. Hillisch, F. A. Gollmick, H. Fritzsche, S. Diekmann, *Biochemistry* **1999**, *38*, 12860–12868.
- [17] a) E. Margeat, A. Kapanidis, P. Tinnefeld, Y. Wang, *Biophys. J.* **2006**, *90*, 1419–1431; b) S. J. Holden, S. Uphoff, J. Hohlbein, D. Yadin, L. L. Reste, O. J. Britton, A. N. Kapanidis, *Biophys. J.* **2010**, *99*, 3102–3111.
- [18] A. N. Kapanidis, N. K. Lee, T. A. Laurence, S. Doose, E. Margeat, S. Weiss, *Proc. Natl. Acad. Sci. USA* **2004**, *101*, 8936–8941.
- [19] N. Lee, A. N. Kapanidis, Y. Wang, X. Michalet, J. Mukhopadhyay, R. H. Ebricht, S. Weiss, *Biophys. J.* **2005**, *88*, 2939–2953.
- [20] A. K. Wozniak, G. F. Schröder, H. Grubmüller, C. A. M. Seidel, F. Oesterheld, *Proc. Natl. Acad. Sci. USA* **2008**, *105*, 18337–18342.
- [21] I. Pastan, S. Adhya, *Bacteriol. Rev.* **1976**, *40*, 527–551.
- [22] E. A. Pyles, J. C. Lee, *Biochemistry* **1996**, *35*, 1162–1172.
- [23] a) R. Schreck, H. Zorbas, E. L. Winnacker, P. A. Baeuerle, *Nucleic Acids Res.* **1990**, *18*, 6497–6502; b) S. Ferrari, V. R. Harley, A. Pontiggia, P. N. Goodfellow, R. Lovell-Badge, M. E. Bianchi, *The EMBO Journal* **1992**, *11*, 4497–4506; c) P. Scaffidi, M. E. Bianchi, *J. Biol. Chem.* **2001**, *276*, 47296–47302.
- [24] S. Uphoff, S. Holden, L. Le Reste, J. Periz, S. v. d. Linde, M. Heilemann, A. N. Kapanidis, *Nat. Methods* **2010**, *7*, 831–836.
- [25] R. H. Ebricht, Y. W. Ebricht, A. Gunasekera, *Nucleic Acids Res.* **1989**, *17*, 10295–10305.
- [26] S. Fredriksson, M. Gullberg, J. Jarvius, C. Olsson, *Nat. Biotechnol.* **2002**, *20*, 473–477.
- [27] A. N. Kapanidis, Y. W. Ebricht, R. H. Ebricht, *J. Am. Chem. Soc.* **2001**, *123*, 12123–12125.

Received: November 4, 2011

Revised: January 13, 2012

Published online on February 24, 2012